CMST 21(1) 29-43 (2015) DOI:10.12921/cmst.2015.21.01.004

An Attempt to Evaluate Accuracy of Diameter of Shallow Blind Holes Drilled in Solid Wood

Bolesław Porankiewicz

Poznan University of Technology
Piotrowo 3, 60-965 Poznań, Poland
E-mail: poranek@amu.edu.pl

Received: 07 July 2014; revised: 13 March 2015; accepted: 13 March 2015; published online: 23 March 2015

Abstract: The paper examines accuracy of low depth, blind holes drilled in a solid wood. Evaluated were statistical dependencies of the exponential form with several double interactions, between shift of average hole diameter series dN and dispersion of holes diameter D_H and parameters of Machine-Tool-Working element (M-T-W) set by drilling solid wood. Significant, nonlinear dependencies of the shift of average hole diameter series dN and dispersion of holes diameter D_H from height of centering spike h_{CS}, drill lateral stiffness E_L, drill bit diameter D_D, radial run out of main cutting edge R_R were found.

Key words: drill bit, hole diameter shift, dispersion of holes diameter, drilling parameters, solid wood, drilling machine

I. INTRODUCTION

Increasing demand on high quality products in wood industry has also forced an increase of dimensional accuracy of wood machining. Dimensional accuracy of drilling processes, described by the shift of average hole diameter series dN and the dispersion of holes diameter D_H is one of criteria of machining quality. In the literature, however, no quantitative relationship between the dN and the D_H and parameters of M-T-W set by drilling wood has been developed yet. Instead of dimensional accuracy, edge quality of holes drilled in wood and wood-based materials was recently the subject of interest [1]. Because of limited stiffness of both tool (typically smaller for closed cutting, in direction perpendicular to tools side surfaces) and work piece, changes in side forces dependent from actual cutting conditions, generate deviations of their mutual position, which results in cutting inaccuracies [4]. This is the reason that parameters describing the M-T-W set influence dimensional accuracy of the drilling process. Dimensional accuracy is important in case of fitted dimensions, especially for mixed and fixed glued connections. Studies in this field were contributory, according to an assumption about the existence of machining tolerances. Parameters describing actual drilling conditions were not taken into consideration. Machining accuracy was evaluated as an average value of hole diameter and standard deviation for undefined cutting conditions. This assumption was employed in works aimed at creation of a limits and fits system for wood industry [3,5,6]. It should be noted that widespread scarcity in the works on woodworking is not determining cutting parameters.

The present study attempts to evaluate quantitative dependencies of shallow blind holes diameter accuracy, defined by the shift of average hole diameter from nominal dimension dN and the dispersion of holes diameter D_H, upon parameters describing M-T-W set during drilling solid wood.

II. EXPERIMENTAL

The holes were drilled in wood of Scotch pine (Pinus sylvestris), with the use of a multi-spindle drilling machine (type DCWGW), and a horizontal milling and drilling machine (type DWJA). Experiments were done by vertical position of the DCWGW 19 working unit. The horizontal oscillations of the DWJA working unit was blocked.

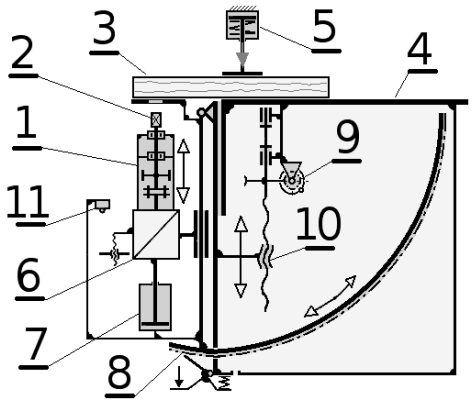

Fig. 1. Scheme of the multi-spindle drilling machine DCWGW 19; 1 – working unit, 2 – drill bit, 3 – working element, 4 – working table, 5 – air cylinders, 6 – electrical motor, 7 – working unit feed air cylinder, 8 – latch mechanism, 9 – snail gear box, 10 – screw mechanism, 11 – end switch

For drilling experiments a random level of independent variables was assumed. New drill bits as well as ones after multiples sharpening were used:

- with and without a centering spike,
- with and without side edges,
- short and long bits, having high and low stiffness E_L,
- small and large diameter D_D,
- with and without main cutting edge bevel angle B_A,
- with a different flute lead angle (maximum rake angle G_F),
- with different tangential S_{TT} and axial S_{RT} side surfaces taper angle,
- with a spiral and straight flute,
- with a cylindrical grip as well as a centering spike together with mounting thread.

The holes were drilled perpendicularly to wide surface of wood specimen, in transversal direction towards wood grains. The following parameters, typical for such drilling operation, were applied. Minimum, average and maximum values were given.

Machining parameters:

- spindle rotational speed $n\langle 2880;\ 6268;\ 10000\rangle$ min^{-1},
- feed per revolution f_R=0.6 mm,
- depth of drilled hole H_O=12 mm.

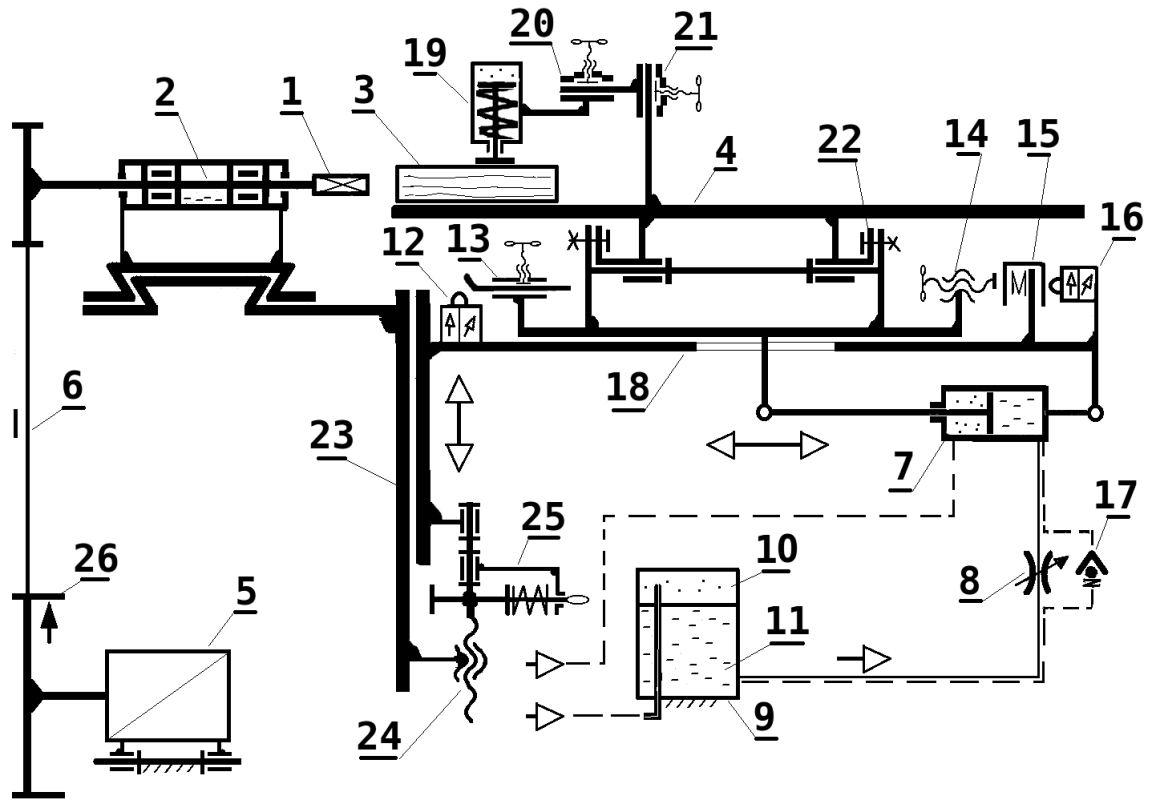

Fig. 2. Scheme of the milling – drilling machine DWJA; 1 – drilling bit, 2 – tool spindle, 3 – working element, 4 – working table, 5 – electrical motor, 6 – belt transmission, 7 – hydraulic – pneumatic cylinder, 8 – throttle valve, 9 – hydraulic – pneumatic reservoir, 10 – air, 11 – oil, 12 – end switch, 13 – adjustable cam, 14 – adjustable back stop, 15 – bumper, 16 – back stop switch, 17 – reversible valve, 18 – horizontal working table support, 19 – single acting fixing air cylinder, 20 – horizontal adjusting and fixing mechanism, 20 – vertical adjusting and fixing mechanism, 22 – table turn mechanism, 23 – vertical working table support, 24 – screw mechanism, 25 – latch mechanism, 26 – electrical motor friction brake

Parameters of the drill bits (Fig. 3):

- drill bit diameter $D_D\langle 6.02;\ 11.54;\ 40.13\rangle$ mm,
- main edge contour rake angle $G_F\langle 0°;\ 12.52°;\ 29°\rangle$,
- main edge contour clearance angle $A_F\langle 2°;\ 15.81°;\ 43°\rangle$,
- main cutting edge bevel angle in base (frontal) plain $B_A\langle 0°;\ 10.83°;\ 62°\rangle$,
- side edge height $h_{SE}\langle 0;\ 0.15;\ 0.8\rangle$ mm,
- side surface arc length $l_{SS}\langle 0;\ 4.43;\ 49.4\rangle$ mm,
- height of centering spike $h_{CS}\langle 0;\ 2.27;\ 6.15\rangle$ mm,
- drill bits working part side surface tangential taper $S_{TT}\langle 0°;\ 2.46°;\ 31°\rangle$
- drill bit working part side surface axial taper S_{AT} $\langle 0;\ 5.11';\ 87'\rangle$ (arc minute),
- lateral stiffness of drill bits mounted in a spindle $E_L\langle 8;\ 72.78;\ 1000\rangle N\cdot \text{mm}^{-1}$,
- number of cutting edges $z = 2$.

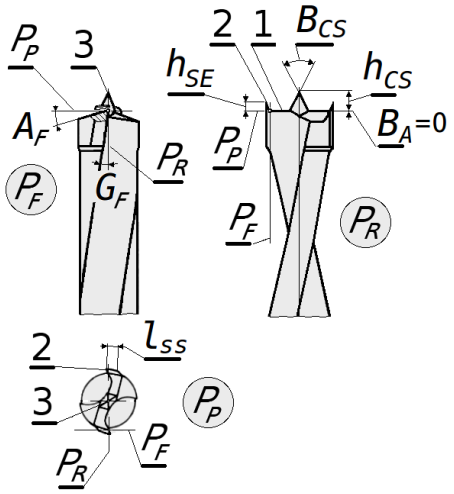

Fig. 3. Stereometrical parameters of the drill bit; 1 – main (face) cutting edge, 2 – side edge, 3 – centering spike, h_{CS} – centering spike height, h_{SE} – side edge height, l_{SS} – side surface arc length, P_F – Working plain, G_F – rake angle of main cutting edge, A_F – clearance of main cutting edge, B_A – bevel angle of main cutting edge, B_{CS} – angle of centering spike, P_R – tool reference plain, P_P – back plain

Parameters of accuracy of the drill bits (Fig. 3)

- radial play of main cutting edge $R_P\langle 0.01\ \ 0.02;\ 0.07\rangle$ mm,
- radial run out of main cutting edge $R_R\langle 0;\ 0.44;\ 1.8\rangle$ mm,
- axial run out of main cutting edge $A_R\langle 0;\ 0.12;\ 0.9\rangle$ mm,
- radial run out of centering spike $R_{RCS}\langle 0;\ 0.08;\ 0.55\rangle$ mm,
- axial run out of side edge $A_{RSE}\langle 0;\ 0.04;\ 0.19\rangle$ mm,
- rake angle difference $dG_F\langle 0°;\ 0.6°;\ 1.8°\rangle$,
- clearance angle differences $dA_F\langle 0°;\ 2.68°;\ 23°\rangle$
- main cutting edge bevel angle in base (frontal) plain difference $dB_A\langle 0°;\ 3.48°;\ 12°\rangle$
- side surface arc length difference $dl_{SS}\langle 0;\ 0.24;\ 3\rangle$ mm.
- centering spike maximum asymmetry angle $dB_{CS}\langle 0°;\ 1.87°;\ 11°\rangle$.

Physical properties of solid wood specimens:

- Brinell hardness $HB\ \langle 0.845;\ 1.84;\ 4.025\rangle$ MPa,
- moisture content 12-15 %.

Dependent variable was an average hole diameter shift from nominal dimension $dN\langle 0;\ 0.31;\ 1.42\rangle$ mm and dispersion of holes diameter $D_H\langle 0.04;\ 0.46;\ 2.75\rangle$ mm.
Experiments were performed for sharp drill bits.
Diameter d_H of 10 shallow, blind holes, drilled for one set of parameters, were measured near the edge in two perpendicular directions, with the use of internal micrometer with accuracy of 0.01 mm, and an average value was taken as a result of the measurement. The hole diameter shift dN was the difference between the average hole diameter d_H and the drill bit diameter D_D. Dispersion of the hole diameter D_H was a standard deviation.

In order to eliminate sorption or desorption dimensional changes of machined wood specimen on holes diameter, measurements were performed just after drilling. The diameter of drill bits D_D was measured with the use of external micrometer with accuracy of 0.01 mm.

The radial run out R_R and axial run out A_R and the radial play R_P of drill bits mounted in the tool spindle were measured with a dial gauge with accuracy of 0.01 mm, fixed with the use of a universal magnetic stand. The lateral stiffness E_L of drill bits mounted in the tool spindle was measured with the use of a dial gauge fixed on a machine table by magnetic stand and hand spring dynamometer.

The other linear and angular parameters of drill bits, like: h_{CS}, h_{SE}, l_{SS}, S_{AT}, S_{TT}, dG_F, B_A, dB_A, A_{RSE} were measured with the use of a tool microscope type BMI, using a prism for drill bits fixing.

The differences dA_F, dG_F, dl_{SS} and dB_A were evaluated for left and right edges.

During the evaluation process of statistical formulas determining quantitative dependencies $dN = f(R_{RCS}, S_{AT}, A_{RSE}, h_{SE}, n, G_F, D_D, h_{CS}, A_R, R_R, E_L, R_P, A_F, dG_F, S_{TT}, HB, dB_{CS})$ and $D_H = f(h_{CS}, E_L, HB, R_R, A_R, R_P, S_{AT}, S_{TT}, R_{RCS}, \text{n}, h_{SE}, G_F, dG_F, A_F, dA_F, B_A, l_{SS})$, linear functions, second order multinomial formulas, as well as power type and exponential functions, with and without possible interactions, were analyzed in preliminary calculations. These relations should fit the experimental matrix by the lowest summation of residuals square S_K, by the lowest S_D, and by the highest correlation coefficient R between predicted and observed values. It is also very important to get the proper influence of variables analyzed, especially in the case of an incomplete experimental matrix. Usually the use of a simpler model results in decreasing approximation quality (larger S_K and S_D, and lower R) and may also re-

verse the impact of lower importance variables. It should be pointed out that the statistical relationship is valid only for ranges of independent variables chosen in the experimental matrix. For some functions, points lying outside the analyzed range of independent variables, especially evaluated for an incomplete experimental matrix, are usually charged by a significant error.

The most adequate models, according to the made assumptions, appeared to be the exponential equation (1) and (2).

$$\begin{aligned} dN =& a_{28} \cdot \exp\left(A_1 + A_2 + A_3 + A_4 + A_5 + A_6\right) \\ &+ a_{29}\ (0 < dN < 1.42)\ (\mathrm{mm}) \end{aligned} \tag{1}$$

$$\begin{aligned} A_1 =& a_1 \cdot dB_{CS} + a_2 \cdot S_{AT} + a_3 \cdot A_{RSE} + a_4 \cdot h_{SE} \\ A_2 =& a_5 \cdot n + a_6 \cdot G_F + a_7 \cdot D_D + a_8 \cdot h_{CS} + a_9 \cdot A_R \\ A_3 =& a_{10} \cdot R_R + a_{11} \cdot E_L + a_{12} \cdot R_P + a_{14} \cdot A_F \\ A_4 =& a_{16} \cdot dG_F \cdot E_L + a_{17} \cdot S_{TT} + a_{19} \cdot R_R \cdot R_P \\ &+ a_{20} \cdot HB + a_{13} \cdot E_L \cdot h_{CS} \\ A_5 =& a_{15} \cdot h_{CS} \cdot R_{RCS} + a_{18} \cdot h_{CS} \cdot HB \\ &+ a_{21} \cdot R_R \cdot E_L + a_{22} \cdot R_{RCS} \cdot R_P + a_{23} \cdot dB_{CS} \cdot R_P \\ A_6 =& a_{24} \cdot dB_A \cdot R_P + a_{25} \cdot dB_{CS} \cdot E_L \\ &+ a_{26} \cdot h_{SE} \cdot R_P + a_{27} \cdot A_{RSE} \cdot h_{SE} \end{aligned}$$

$$\begin{aligned} D_H =& b_{34} \cdot \exp\left(B_1 + B_2 + B_3 + B_4 + B_5 + B_6\right) \\ &+ b_{35}\ (0.04 < D_H < 2.75)\ (\mathrm{mm}) \end{aligned} \tag{2}$$

$$\begin{aligned} B_1 =& b_1 \cdot dB_{CS} \cdot E_L^{a28} + b_2 \cdot S_{AT} + b_3 \cdot A_{RSE} \cdot E_L^{a29} \\ &+ b_4 \cdot h_{SE} \\ B_2 =& b_5 \cdot n + b_6 \cdot G_F + b_7 \cdot D_D + b_8 \cdot h_{CS} \\ B_3 =& b_9 \cdot A_R + b_{10} \cdot R_R^{b24} \cdot h_{CS}^{b30} + b_{11} \cdot E_L^{b31} \\ &+ b_{12} \cdot R_P \cdot E_L^{b33} \\ B_4 =& b_{13} \cdot R_{RCS} + b_{14} \cdot A_F + b_{15} \cdot dA_F + b_{16} \cdot dG_F \\ &+ b_{17} \cdot S_{TT} \\ B_5 =& b_{19} \cdot B_A + b_{20} \cdot HB \cdot h_{CS}^{b32} + b_{18} \cdot h_{CS}^{b22} \cdot E_L^{b23} \\ B_6 =& b_{21} \cdot h_{CS} \cdot l_{SS} + b_{25} \cdot h_{CS}^{b26} \cdot R_P^{b27}, \end{aligned}$$

where: $\exp(x) = e^x$ and $e = 2.7182818$.

Estimators, also called coefficients of regression equation, were evaluated from an incomplete experimental matrix having 145 data points. During the evaluation process of chosen mathematical models, unimportant or low important estimators were eliminatedusing coefficient of relative importance C_{RI}, defined by equation (3), by assumption $C_{RI} > 0.1$

$$C_{RI} = (S_K + S_{KOk}) \cdot S_K^{-1} \cdot 100\ (\%) \tag{3}$$

In equation (3) the new terms are:

- S_{K0k} – summation of square of residuals, by estimator $a_k = 0$,
- a_k – estimator of the number k in empirical formula evaluated.

Summation of square of residuals S_K, standard deviation of residuals S_R, correlation coefficient R and the square of correlation coefficient R^2, between predicted and observed values were used for characterization of approximation quality [2].

Calculation was performed at Poznań Supercomputing and Networking Center (PCSS) on a SGI Altix 3700 machine, using an optimization program, prepared by the author, based on the least square method. For the defined mathematical formula and initial approximation, this program (Fig. 4) is searching, in an iterative manner, for a solution with minimum summation of square of residuals S_K. Preferred values of initial estimators can be any small numbers. For linear (LF), polinominal (PNF) as well as trygonometrical functions (TF) it can be just 1.0. For power (PF) and exponential functions (EF) can be respectively 0.1 and 0.001 or smaller, depending on the value of independent variables. Corrected estimators for every loop are determined from a defined range of searches, using gradient and Monte Carlo methods as well as several combinations of them. Construction of the program allows adding new parts to the statistical formula. It is efficient to start calculation from a simple equation and stepwise add new parts. It is also possible to remove parts of the formula due to the lack of importance. In case of reaching the local minimum or out of range instance, calculation needs interference. Depending on the size of an experimental matrix, for LF, PNF and TF cases, a final solution can be found after less than 10^8 iterations. For cases PF and EF, especially for a large number of independent variables, interactions and number of tests, as well as in case of presence of local minimums, the necessary number of iterations can be much higher (10^{13}).

III. RESULTS AND DISCUSSION

Appendix contains a collection of estimators and coefficients of relative importance for equations (1) and (2).

Approximation quality of the fit of the equation (1) can be characterized by the quantifiers: $S_K = 2.06$, $R = 0.89$; $R^2 = 0.80$; $S_R = 0.12$ mm, and was also illustrated in Fig. 5. The final solution was obtained after the number of iteration of 5.810^8. In formula (1) twelve interactions were found: $-dG_F \cdot E_L$, $-R_R \cdot R_P$, $E_L \cdot h_{CS}$,

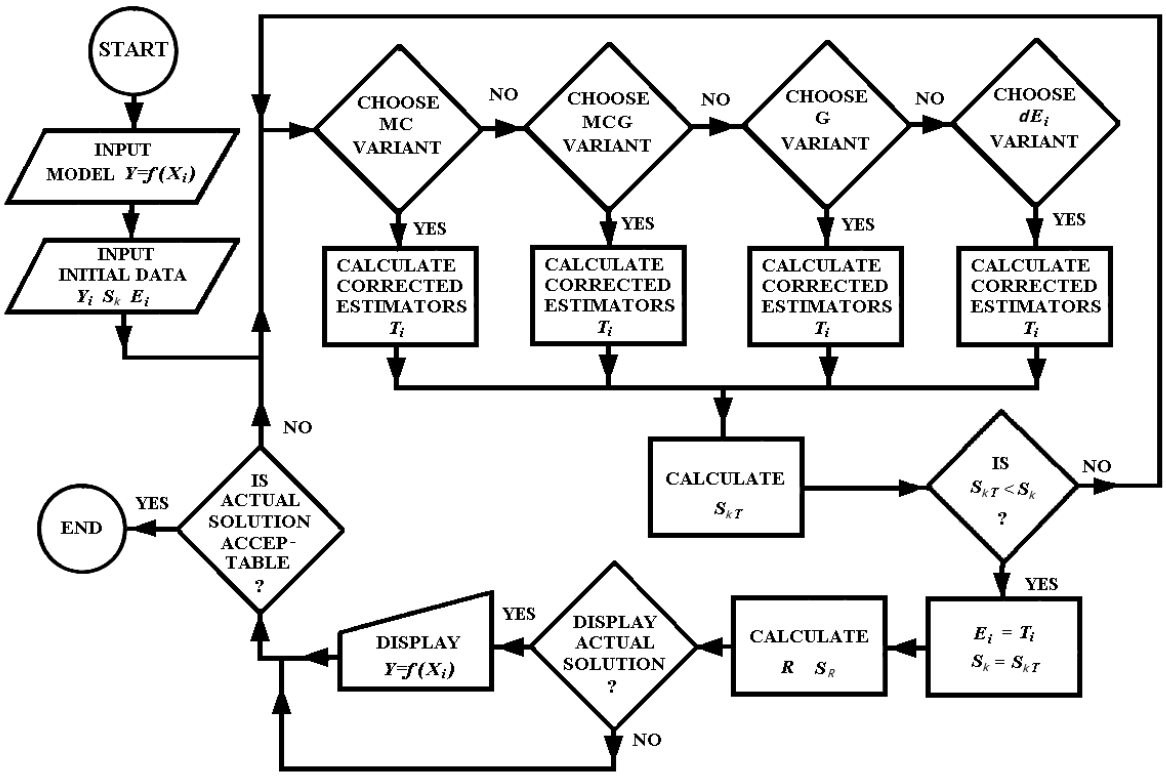

Fig. 4. Flowing chart of the optimization program; variants: MC – Monte Carlo, G – gradient, MCG – combined MC and G, S_K – summation of square of residuals, R – correlation coefficient, S_R – standard deviation of residuals

$h_{CS}{\cdot}R_{RCS}$, $-h_{CS}{\cdot}HB$, $R_R{\cdot}E_L$, $-h_{CS}{\cdot}R_{RCS}$, $dB_{CS}{\cdot}R_P$, $-dB_A \cdot R_P$, $dB_{CS} \cdot E_L$, $-h_{SE} \cdot R_P$ and $A_{RSE} \cdot h_{SE}$. The most involved independent variables in the interactions are: transversal stiffness E_L, height of the centering spike h_{CS} and – radial play R_P.

The approximation quality of the fit of the equation (2) can be characterized by quantifiers: $S_K = 4.83$, $R = 0.92$, $R^2 = 0.84$, $S_D = 0.18$ mm, and was also illustrated in Fig. 6. The final result was obtained after the number of iteration of 2.210^9.

In the formula (2) eight interactions can be seen: $dB_{CS} \cdot E_L$, $-A_{RSE}{\cdot}E_L$, $R_R{\cdot}h_{CS}$, $R_P{\cdot}E_L$, $-HB{\cdot}h_{CS}$, $h_{CS}{\cdot}E_L$, $h_{CS} \cdot l_{SS}$, $h_{CS} \cdot R_P$. The most involved independent variables in the interactions are: transversal stiffness of the drill bit E_L, height of the centering spike h_{CS}, radial run out R_R and radial play R_P.

Figs. 5 and 6 show asymmetric distribution of measuring points of the dN and D_H. More than 60% of the dN are lower than 0.25 mm. Differences between the observed and predicted values are low, for several ranges of the dN and D_H. For some measuring points these differences are much larger. Uncontrolled variation of the dN and D_H. (Figs. 5 and 6) may have a source in random, unsymmetrical distribution of wood properties in the cutting region. It is also possible an influence of not taken into account independent variables or interactions. The analyzed problem looks very complex. However, most of variation of the dN and D_H, considered in the past as machining tolerances [3,5,6] was taken into account in the formulas (1) and (2).

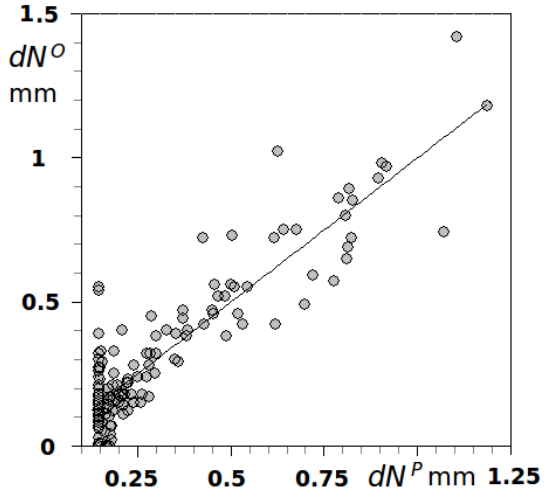

Fig. 5. Plot of observed hole diameter shift dN^O against predicted dN^P value

Fig. 7 shows that the hole diameter shift dN strongly, non-linearly depends upon the S_{AT} and the dB_{CS}. With

a reduction of the S_{AT} and the dB_{CS} the dN significantly increased. The dependence of the dN from both variables by the $S_{AT} > 40'$ (where: $'$ means angle minute) was negligibly small.

Fig. 8 shows the dN dependency from the A_{RSE} and the h_{SE}. An increase of the h_{SE}, together with an decrease of the A_{RSE}, significantly increased the dN, by strong increasing tendency.

Fig. 9 reveals slight, positive dependency of the dN from increasing of the n and the G_F.

Fig. 10 shows hole diameter shift dN strong, non-linear dependency from the h_{CS} and the D_D. A decrease of the h_{CS} and an increase of the D_D increased the average hole diameter shift dN. Reduction of the h_{CS} caused significant enlargement of the dN, more intensive with increasing of the D_D.

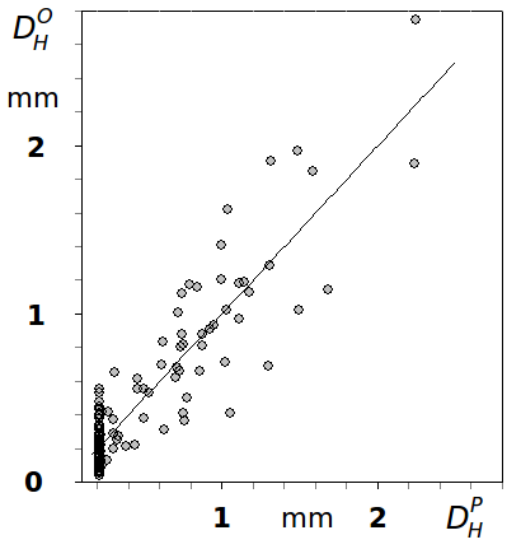

Fig. 6. The plot of observed hole diameter shift ${D_H}^O$ against predicted ${D_H}^P$ value

Fig. 11 shows influence of the R_R and the A_R on the dN. It can be seen that the dN strongly, nonlinearly increased with an enlargement of the R_R for the whole range of variation of the A_R. However, for low values of the R_R the influence of the A_R on the dN was negligibly small.

Fig. 12 shows dependency of the dN upon the E_L and the R_P. It can be seen that the dN strongly, nonlinearly increased with an increase of the E_L, for the whole range of variation of the R_P. The influence of the R_P on the dN, for low values of the E_L was negligibly small.

Fig. 13 shows dependency of the dN from the A_F and R_{RCS}. With increasing tendency, an enlargement of the R_{RCS}, and decreasing of the A_F the dN increased. The influence of the A_F was lower and disappeared starting from $R_{RCS} < 0.1$ mm.

Fig. 14 depicts influence of the dB_A and the S_{TT} on the dN. An increase of the dB_A results in slight decreasing of the dN. An increase of the S_{TT} slightly increased the dN.

Fig. 15 shows dependence of the dN upon the HB and the dG_F. An enlargement of the HB decreased the dN. The relation $dN = f(dG_F)$ was much smaller. An increase of the dG_F results in slight decreasing of the dN.

Because of a large number of interactions: $-dG_F \cdot E_L$, $-R_R \cdot R_P$, $E_L \cdot h_{CS}$, $h_{CS} \cdot R_{RCS}$, $-h_{CS} \cdot HB$, $R_R \cdot E_L$, $-h_{CS} \cdot R_{RCS}$, $dB_{CS} \cdot R_P$, $-dB_A \cdot R_P$, $dB_{CS} \cdot E_L$, $-h_{SE} \cdot R_P$ and $A_{RSE} \cdot h_{SE}$, dependencies shown in Figs. 7-15 may differ for another set of independent variables.

No correlation between the dN and following independent variables: dA_F, B_A, l_{SS}, dl_{SS} was found.

Fig. 16 shows that the D_H was strongly depended upon the h_{SE}. With an increase of the h_{SE} and the A_{RSE} the D_H significantly decreased. The side edge seems to have a stabilization effect on the a drill during work.

The hole diameter shift D_H was strongly, non-linearly dependent upon the n and the G_F, which can be seen in Fig. 17. An increase of the n and the G_F decreased the average hole diameter dispersion D_H. With an increase of the n the D_H slightly dropped down. Increasing accuracy of the drilling process with increase of the n and G_F can be associated with shortening of cutting (larger n) and lowering cutting forces (lower G_F).

The hole diameter shift D_H was strongly, non-linearly dependent upon the h_{CS} and the D_D, which can be seen in Fig. 18. An increase of the h_{CS} and the D_D increased the dispersion of hole diameter D_H. With an decrease of the h_{CS} the D_H slightly dropped down. This relation was more intensive for large D_D and h_{CS}. For low h_{CS} the relation $D_H = f(D_D)$ was negligibly small.

The hole diameter shift D_H was strongly, non-linearly depend upon the R_R, which can be seen in Fig. 19. An increase of the R_R increased the dispersion of hole diameter D_H. This influence of the relation A_R was negligibly small for low values of the R_R.

Fig. 20 shows dependency of the R_P upon the E_L. It can be seen that the D_H strongly, nonlinearly decreased with an increase of the R_P, especially for larger values of the E_L. For low E_L the relation $D_H = f(R_P)$ was negligibly small.

Fig. 21 shows dependency of the D_H upon the A_F and the R_{RCS}. It can be seen that the D_H nonlinearly decreased with an increase of the A_F. The influence of the R_{RCS} on the D_h was very small.

Fig. 22 shows the D_H dependency on the dG_F and the dA_F. With an increase of the dG_F the D_H decreased. The influence of the dA_F was opposite and lower, especially for the highest dG_F.

Fig. 23 depicts the influence of the S_{TT} and the B_A on the D_H. An increase of the S_{TT} and of the B_A results in slightly increasing of the D_H.

Fig. 24 shows the influence of the HB and the h_{CS} on the D_H. An increase of the h_{CS} slightly decreased the D_H for large values of the HB. For small values of the HB, increasing value of the h_{CS} rapidly increasing of the D_H can be seen. For high h_{CS} and the HB the relation $D_H = f(h_{CS}, HB)$ was negligibly small.

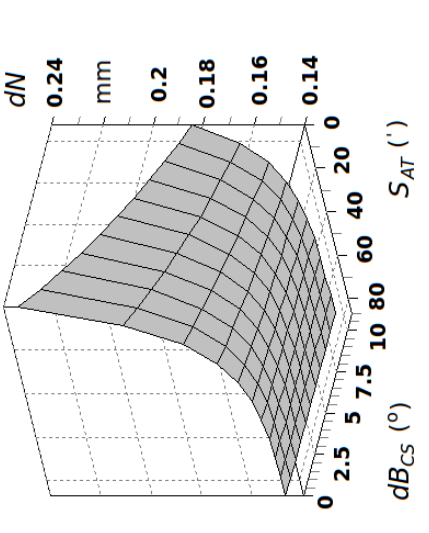

Fig. 7. Plot of relation between the average hole diameter shift dN and the centering spike maximum asymmetry angle dB_{CS} (°) and the drill bit working part side surface axial taper S_{AT} (′ arc min.); axial run out of side edge $A_{RSE} = 0.19$ mm; side edge height $h_{SE} = 0.8$ mm; spindle rotational speed $n = 2880$ min^{-1}; main edge contour rake angle G_F=0°; height of centering spike $h_{CS} = 0.01$ mm; drill bit diameter $D_D = 11$ mm; axial run out of main cutting edge $A_R = 0.1$ mm; radial run out of main cutting edge $R_R = 0.4$ mm; lateral stiffness of drill bits mounted in a spindle E_L=72 Nmm^{-1}; radial play of main cutting edge $R_P = 0.02$ mm; radial run out of centering spike $R_{RCS} = 0.08$ mm; main edge contour clearance angle $A_F = 15°$; rake angle differences $dG_F = 0.6°$; drill bits working part side surface tangential taper $S_{TT} = 2°$; main cutting edge bevel angle in base plain difference $dB_A = 3°$; Brinell hardness $HB = 4$ MPa

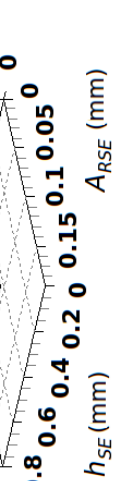

Fig. 8. Plot of relation between average hole diameter shift dN and the axial run out of side edge A_{RSE} and the side edge height h_{SE}; centering spike maximum asymmetry angle $dB_{CS} = 1.9$ mm; drill bit working part side surface axial taper $S_{AT} = 5'$; spindle rotational speed $n = 2880$ min^{-1}; main edge contour rake angle G_F=0°; height of centering spike $h_{CS} = 0.01$ mm; drill bit diameter $D_D = 11$ mm; axial run out of main cutting edge $A_R = 0.1$ mm; radial run out of main cutting edge $R_R = 0.4$ mm; lateral stiffness of drill bits mounted in a spindle E_L=8 N mm^{-1}; radial play of main cutting edge $R_P = 0.07$ mm; radial run out of centering spike $R_{RCS} = 0.08$ mm; main edge contour clearance angle $A_F = 15°$; rake angle differences $dG_F = 0.6°$; drill bits working part side surface tangential taper $S_{TT} = 2°$; main cutting edge bevel angle in base plain difference $dB_A = 3°$; Brinell hardness $HB = 4$ MPa

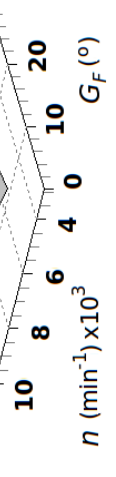

Fig. 9. Plot of relation between the hole diameter shift dN and the spindle rotational speed n and the main edge contour rake angle G_F; centering spike maximum asymmetry angle $dB_{CS} = 1.9$ mm; drill bit working part side surface axial taper drill bit working part side surface axial taper $S_{AT} = 5'$; axial run out of side edge $A_{RSE} = 0.04$ mm; side edge height $h_{SE} = 0.8$ mm; height of centering spike $h_{CS} = 2$ mm; drill bit diameter $D_D = 11$ mm; axial run out of main cutting edge $A_R = 0.1$ mm; radial run out of main cutting edge $R_R = 0.4$ mm; lateral stiffness of drill bits mounted in a spindle $E_L = 72$ N mm^{-1}; radial play of main cutting edge $R_P = 0.02$ mm; radial run out of centering spike $R_{RCS} = 0.08$ mm; main edge contour clearance angle $A_F = 15°$; rake angle differences $dG_F = 0.6°$; drill bits working part side surface tangential taper $S_{TT} = 2°$; main cutting edge bevel angle in base plain difference $dB_A = 3°$; Brinell hardness $HB = 4$ MPa

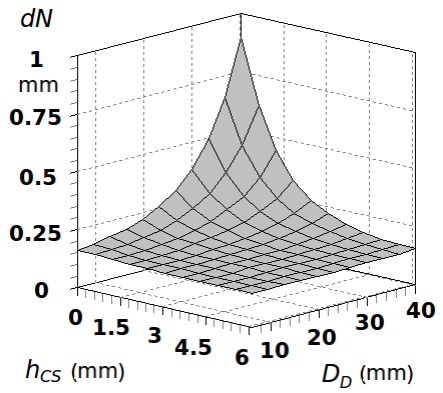

Fig. 10. Plot of relation between the hole diameter shift dN and the drill bit diameter D_D and the height of centering spike h_{CS}; centering spike maximum asymmetry angle $dB_{CS} = 1.9$ mm; drill bit working part side surface axial taper $S_{AT} = 5'$; axial run out of side edge $A_{RSE} = 0.4$ mm; side edge height $h_{SE} = 0.8$ mm; spindle rotational speed $n = 2880$ min^{-1}; main edge contour rake angle $G_F = 12°$; axial run out of main cutting edge $A_R = 0.1$ mm; radial run out of main cutting edge $R_R = 0.4$ mm; lateral stiffness of drill bits mounted in a spindle $E_L = 140$ N mm^{-1}; radial play of main cutting edge $R_P = 0.02$ mm; radial run out of centering spike $R_{RCS} = 0.08$ mm; main edge contour clearance angle $A_F = 15°$; rake angle differences $dG_F = 0.6°$; drill bits working part side surface tangential taper $S_{TT} = 2°$; main cutting edge bevel angle in base plain difference $dB_A = 3°$; Brinell hardness $HB = 4$ MPa

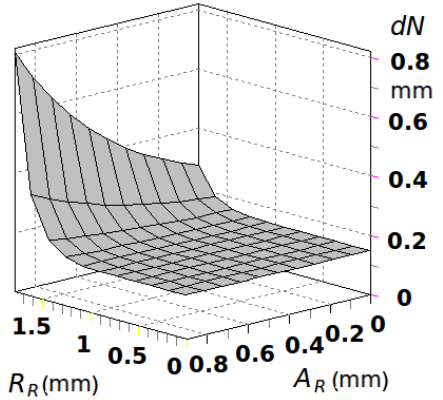

Fig. 11. Plot of relation between the hole diameter shift dN and the axial run out of main cutting edge A_R and the radial run out of main cutting edge R_R; centering spike maximum asymmetry angle $dB_{CS} = 1.9$ mm; drill bit working part side surface axial taper $S_{AT} = 5'$; axial run out of side edge $A_{RSE} = 0$ mm; side edge height $h_{SE} = 0$ mm; spindle rotational speed $n = 2880$ min^{-1}; main edge contour rake angle $G_F = 29°$; height of centering spike $h_{CS} = 6$ mm; drill bit diameter $D_D = 11$ mm; lateral stiffness of drill bits mounted in a spindle $E_L = 42$ N mm^{-1}; radial play of main cutting edge $R_P = 0.01$ mm; radial run out of centering spike $R_{RCS} = 0.08$ mm; main edge contour clearance angle $A_F = 15°$; rake angle differences $dG_F = 0.6°$; drill bits working part side surface tangential taper $S_{TT} = 2°$; main cutting edge bevel angle in base plain difference $dB_A = 3°$; Brinell hardness $HB = 4$ MPa

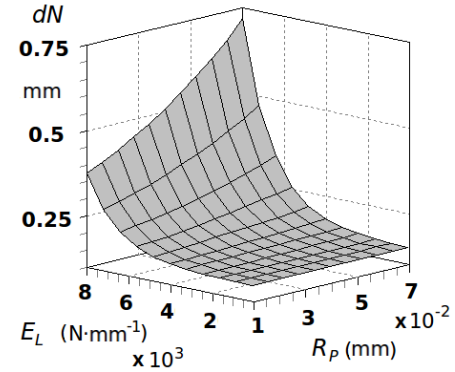

Fig. 12. Plot of relation between the hole diameter shift dN and the lateral stiffness of drill bits mounted in a spindle E_L and the radial play of main cutting edge R_P; centering spike maximum asymmetry angle $dB_{CS} = 1.9$ mm; drill bit working part side surface axial taper $S_{AT} = 5'$; axial run out of side edge $A_{RSE} = 0.1$ mm; side edge height $h_{SE} = 0.1$ mm; spindle rotational speed $n = 2880$ min^{-1}; main edge contour rake angle main edge contour rake angle $G_F = 0°$; height of centering spike $h_{CS} = 1.5$ mm; drill bit diameter $D_D = 11$ mm; axial run out of main cutting edge $A_R = 0.1$ mm; radial run out of main cutting edge $R_R = 0.6$ mm; radial run out of centering spike $R_{RCS} = 0.08$ mm; main edge contour clearance angle $A_F = 15°$; rake angle differences $dG_F = 0.6°$; drill bits working part side surface tangential taper $S_{TT} = 2°$; main cutting edge bevel angle in base plain difference $dB_A = 3°$; Brinell hardness $HB = 4$ MPa

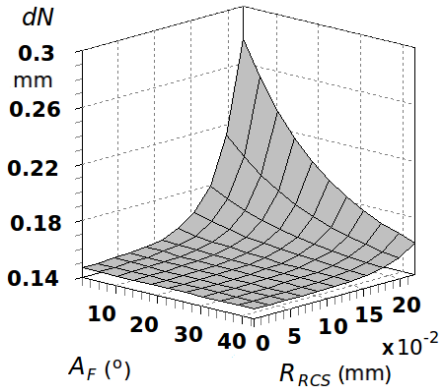

Fig. 13. Plot of relation between the hole diameter shift dN and the radial run out of centering spike R_{RCS} and the main edge contour clearance angle A_F; centering spike maximum asymmetry angle dB_{CS}=1.9 mm; drill bit working part side surface axial taper $S_{AT} = 5'$; axial run out of side edge $A_{RSE} = 0.04$ mm; side edge height $h_{SE} = 0.8$ mm; spindle rotational speed $n = 2880$ min^{-1}; main edge contour rake angle $G_F = 12°$; height of centering spike $h_{CS} = 6$ mm; drill bit diameter $D_D = 11$ mm; axial run out of main cutting edge $A_R = 0.1$ mm; radial run out of main cutting edge $R_R = 0.4$ mm; lateral stiffness of drill bits mounted in a spindle $E_L = 8$ N mm^{-1}; radial play of main cutting edge $R_P = 0.02$ mm; rake angle differences $dG_F = 0.6°$; drill bits working part side surface tangential taper $S_{TT} = 2°$; main cutting edge bevel angle in base plain difference $dB_A = 3°$; Brinell hardness $HB = 4$ MPa

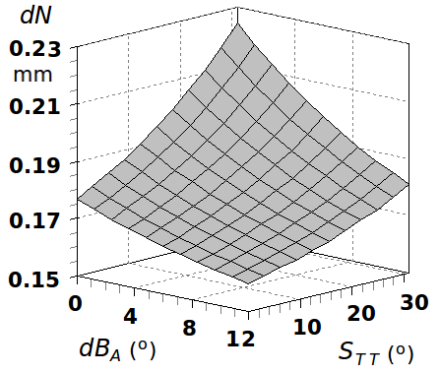

Fig. 14. Plot of relation between the hole diameter shift dN and the drill bits working part side surface tangential taper S_{TT} and the main cutting edge bevel angle in base plain difference dB_A; centering spike maximum asymmetry angle dB_{CS}=1.9 mm; drill bit working part side surface axial taper $S_{AT} = 5'$; axial run out of side edge $A_{RSE} = 0.04$ mm; side edge height $h_{SE} = 0.8$ mm; spindle rotational speed $n = 2880$ min^{-1}; main edge contour rake angle $G_F = 12°$; height of centering spike $h_{CS} = 1$ mm; drill bit diameter $D_D = 11$ mm; axial run out of main cutting edge $A_R = 0.1$ mm; radial run out of main cutting edge $R_R = 0.4$ mm; lateral stiffness of drill bits mounted in a spindle $E_L = 72$ N mm^{-1}; radial play of main cutting edge $R_P = 0.02$ mm; radial run out of centering spike $R_{RCS} = 0.08$ mm; main edge contour clearance angle $A_F = 15°$; rake angle differences $dG_F = 0.6°$; Brinell hardness $HB = 4$ MPa

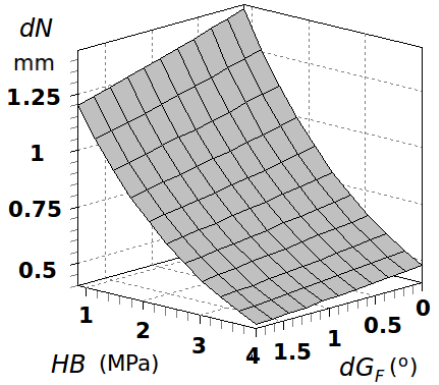

Fig. 15. Plot of relation between the hole diameter shift dN and the Brinell hardness HB and the rake angle differences dG_F, according to equation (3); $dB_{CS} = 1.9$ mm; drill bit working part side surface axial taper $S_{AT} = 5'$; axial run out of side edge $A_{RSE} = 0.04$ mm; side edge height $h_{SE} = 0.8$ mm; spindle rotational speed $n = 2880$ min^{-1}; main edge contour rake angle $G_F = 0°$; height of centering spike $h_{CS} = 1.5$ mm; drill bit diameter $D_D = 6$ mm; axial run out of main cutting edge $A_R = 0.2$ mm; radial run out of main cutting edge $R_R = 0.2$ mm; lateral stiffness of drill bits mounted in a spindle $E_L = 8$ N mm^{-1}; radial play of main cutting edge $R_P = 0.01$ mm; radial run out of centering spike $R_{RCS} = 0$ mm; main edge contour clearance angle $A_F = °$; drill bits working part side surface tangential taper $S_{TT} = 0°$; main cutting edge bevel angle in base plain difference $dB_A = 0°$

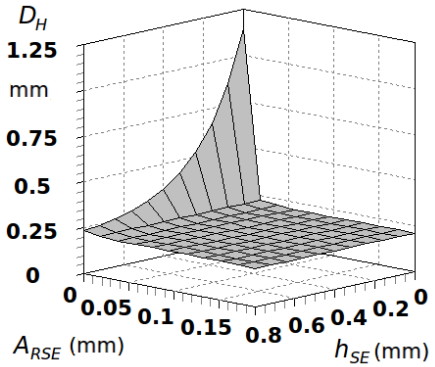

Fig. 16. The plot of relation between the dispersion of hole diameter D_H and the axial run out of side edge A_{RSE} and the side edge height h_{SE}; centering spike maximum asymmetry angle dB_{CS}=11 mm; drill bit working part side surface axial taper S_{AT}=5'; spindle rotational speed $n = 2880$ min^{-1}; main edge contour rake angle $G_F = 0°$; height of centering spike $h_{CS} = 0.2$ mm; drill bit diameter $D_D = 11$ mm; axial run out of main cutting edge $A_R = 0.4$ mm; radial run out of main cutting edge $R_R = 0.6$ mm; lateral stiffness of drill bits mounted in a spindle $E_L = 72\ \text{N mm}^{-1}$; radial play of main cutting edge $R_P = 0.02$ mm; radial run out of centering spike $R_{RCS} = 0.08$ mm; main edge contour clearance angle $A_F = 15°$; clearance angle differences $dA_F = 2°$; rake angle differences $dG_F = 0.6°$; drill bits working part side surface tangential taper $S_{TT} = 2°$; main cutting edge bevel angle in base plain difference $dB_A = 3°$; main cutting edge bevel angle in base plain $B_A = 10°$; Brinell hardness $HB = 4$ MPa

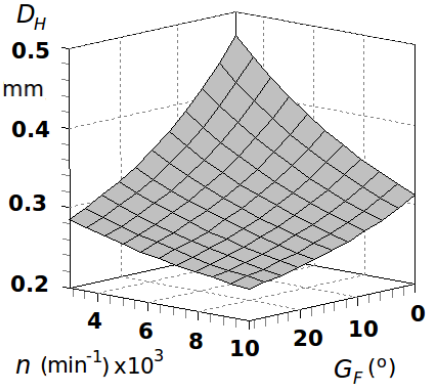

Fig. 17. The plot of relation between the dispersion of hole diameter D_H and the spindle rotational speed n and the main edge contour rake angle G_F; centering spike maximum asymmetry angle $dB_{CS} = 0$ mm; drill bit working part side surface axial taper $S_{AT} = 87'$; axial run out of side edge $A_{RSE} = 0$ mm; side edge height $h_{SE} = 0$ mm; height of centering spike $h_{CS} = 0.01$ mm; drill bit diameter $D_D = 8$ mm; axial run out of main cutting edge $A_R = 0.9$ mm; radial run out of main cutting edge $R_R = 1.8$ mm; lateral stiffness of drill bits mounted in a spindle $E_L = 90\ \text{N mm}^{-1}$; radial play of main cutting edge $R_P = 0.07$ mm; radial run out of centering spike $R_{RCS} = 0$ mm; main edge contour clearance angle $A_F = 43°$; clearance angle differences $dA_F = 23°$; rake angle differences $dG_F = 1.8°$; drill bits working part side surface tangential taper $S_{TT} = 31°$; main cutting edge bevel angle in base plain difference $dB_A = 3°$; main cutting edge bevel angle in base plain $B_A = 0°$; Brinell hardness $HB = 4$ MPa

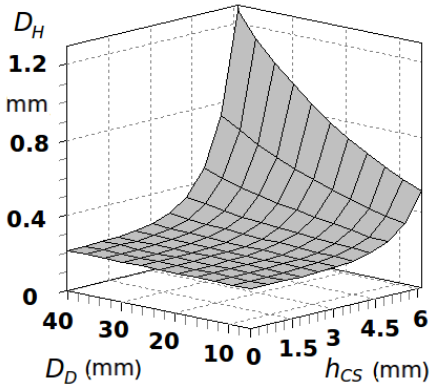

Fig. 18. The plot of relation between the dispersion of hole diameter D_H and the drill bit diameter D_D and the height of centering spike h_{CS}, according to equation (3); $dB_{CS} = 11$ mm; drill bit working part side surface axial taper $S_{AT} = 5'$; axial run out of side edge $A_{RSE} = 0.04$ mm; side edge height $h_{SE} = 0.2$ mm; spindle rotational speed $n = 2880$ min^{-1}; main edge contour rake angle $G_F = 12°$; axial run out of main cutting edge $A_R = 0.4$ mm; radial run out of main cutting edge $R_R = 0.6$ mm; lateral stiffness of drill bits mounted in a spindle $E_L = 8\ \text{N mm}^{-1}$; radial play of main cutting edge $R_P = 0.02$ mm; radial run out of centering spike $R_{RCS} = 0.08$ mm; $A_F = 15°$; $dA_F = 2°$; rake angle differences $dG_F = 0.6°$; drill bits working part side surface tangential taper $S_{TT} = 2°$; main cutting edge bevel angle in base plain difference $dB_A = 3°$; main cutting edge bevel angle in base plain $B_A = 10°$; Brinell hardness $HB = 1$ MPa

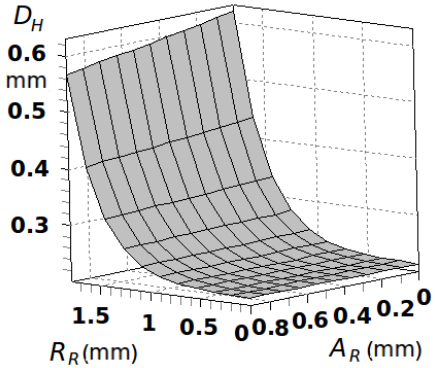

Fig. 19. The plot of relation between the dispersion of hole diameter D_H and the radial run out of main cutting edge R_R and the axial run out of main cutting edge A_R; centering spike maximum asymmetry angle $dB_{CS} = 11$ mm; drill bit working part side surface axial taper $S_{AT} = 5'$; axial run out of side edge $A_{RSE} = 0.04$ mm; side edge height $h_{SE} = 0.8$ mm; spindle rotational speed $n = 2880$ min^{-1}; main edge contour rake angle $G_F = 12°$; height of centering spike $h_{CS} = 0.1$ mm; drill bit diameter $D_D = 12$ mm; lateral stiffness of drill bits mounted in a spindle $E_L = 150$ N mm^{-1}; radial play of main cutting edge $R_P = 0.02$ mm; radial run out of centering spike $R_{RCS} = 0.08$ mm; main edge contour clearance angle $A_F = 15°$; clearance angle differences $dA_F = 2°$; $dG_F = 0.6°$; drill bits working part side surface tangential taper $S_{TT} = 2°$; main cutting edge bevel angle in base plain difference $dB_A = 3°$; main cutting edge bevel angle in base plain $B_A = 10°$; Brinell hardness $HB = 0.85$ MPa

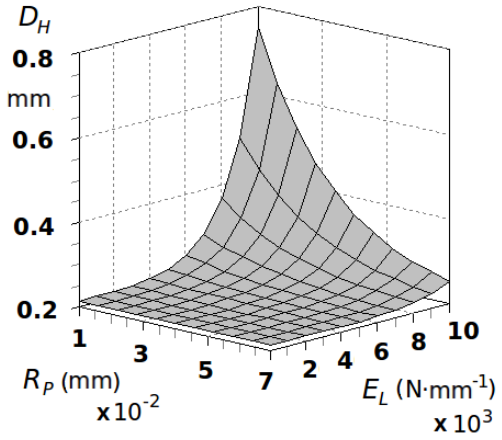

Fig. 20. The plot of relation between the dispersion of hole diameter D_H and the radial play of main cutting edge R_P and the lateral stiffness of drill bits mounted in a spindle E_L; centering spike maximum asymmetry angle $dB_{CS} = 11$ mm; drill bit working part side surface axial taper $S_{AT} = 5'$; axial run out of side edge $A_{RSE} = 0.04$ mm; side edge height $h_{SE} = 0.1$ mm; spindle rotational speed n=2880 min^{-1}; main edge contour rake angle G_F=12°; drill bit diameter $D_D = 11$ mm; $h_{CS} = 1.5$ mm; axial run out of main cutting edge $A_R = 0.1$ mm; radial run out of main cutting edge $R_R = 0.4$ mm; radial run out of centering spike $R_{RCS} = 0.08$ mm; main edge contour clearance angle A_F=15°; clearance angle differences $dA_F = 2°$; rake angle differences $dG_F = 0.6°$; drill bits working part side surface tangential taper $S_{TT} = 2°$; main cutting edge bevel angle in base plain difference $dB_A = 3°$; main cutting edge bevel angle in base plain $B_A = 10°$; Brinell hardness $HB = 0.85$ MPa centering spike maximum asymmetry angle $dB_{CS} = 11$ mm; drill bit working part side surface axial taper $S_{AT} = 87'$; axial run out of side edge $A_{RSE} = 0$ mm; side edge height $h_{SE} = 0$ mm; spindle rotational speed $n = 2880$ min^{-1}; main edge contour rake angle G_F=0°; height of centering spike h_{CS}; drill bit diameter $D_D = 6$ mm; axial run out of main cutting edge $A_R = 0.2$ mm; radial run out of main cutting edge $R_R = 0.4$ mm; lateral stiffness of drill bits mounted in a spindle $E_L = 72$ N mm^{-1}; radial play of main cutting edge $R_P = 0.05$ mm; radial run out of centering spike $R_{RCS} = 0.55$ mm; main edge contour clearance angle $A_F = 43°$; clearance angle differences $dA_F = 23°$; rake angle differences $dG_F = 1.8°$; drill bits working part side surface tangential taper $S_{TT} = 0°$; main cutting edge bevel angle in base plain difference $dB_A = 12°$; main cutting edge bevel angle in base plain $B_A = 31°$; Brinell hardness HB

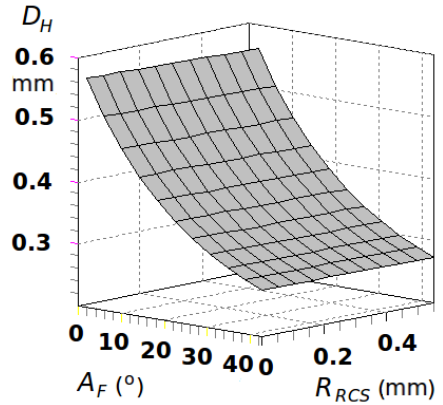

Fig. 21. The plot of relation between the dispersion of hole diameter D_H and the radial run out of centering spike R_{RCS} and the main edge contour clearance angle A_F; centering spike maximum asymmetry angle $dB_{CS} = 11$ mm; drill bit working part side surface axial taper $S_{AT} = 5'$; axial run out of side edge $A_{RSE} = 0.04$ mm; side edge height $h_{SE} = 0.2$ mm; spindle rotational speed $n = 2880$ min^{-1}; main edge contour rake angle $G_F = 12°$; drill bit diameter $D_D = 11$ mm; height of centering spike $h_{CS} = 4$ mm; axial run out of main cutting edge $A_R = 0.1$ mm; radial run out of main cutting edge $R_R = 0.4$ mm; lateral stiffness of drill bits mounted in a spindle $E_L = 72$ N mm^{-1}; radial play of main cutting edge $R_P = 0.02$ mm; clearance angle differences $dA_F = 2°$; rake angle differences $dG_F = 0.6°$; drill bits working part side surface tangential taper $S_{TT} = 2°$; main cutting edge bevel angle in base plain difference $dB_A = 3°$; main cutting edge bevel angle in base plain $B_A = 10°$; Brinell hardness $HB = 0.85$ MPa

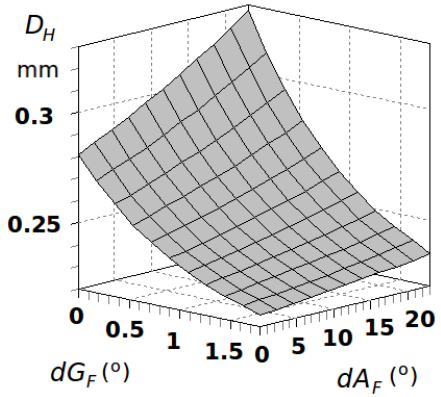

Fig. 22. The plot of relation between the dispersion of hole diameter D_H and the clearance angle differences dA_F and the rake angle differences dG_F; centering spike maximum asymmetry angle dB_{CS}=11 mm; drill bit working part side surface axial taper $S_{AT} = 5'$; axial run out of side edge $A_{RSE} = 0.19$ mm; side edge height $h_{SE} = 0.8$ mm; spindle rotational speed $n = 2880$ min^{-1}; main edge contour rake angle $G_F = 12°$; drill bit diameter $D_D = 11$ mm; height of centering spike $h_{CS} = 5$ mm; axial run out of main cutting edge $A_R = 0.2$ mm; radial run out of main cutting edge $R_R = 0.6$ mm; lateral stiffness of drill bits mounted in a spindle $E_L = 72$ N mm^{-1}; radial play of main cutting edge $R_P = 0.02$ mm; radial run out of centering spike $R_{RCS} = 0.08$ mm; main edge contour clearance angle $A_F = 15°$; drill bits working part side surface tangential taper $S_{TT} = 2°$; main cutting edge bevel angle in base plain difference $dB_A = 3°$; main cutting edge bevel angle in base plain $B_A = 10°$; Brinell hardness $HB = 0.85$ MPa

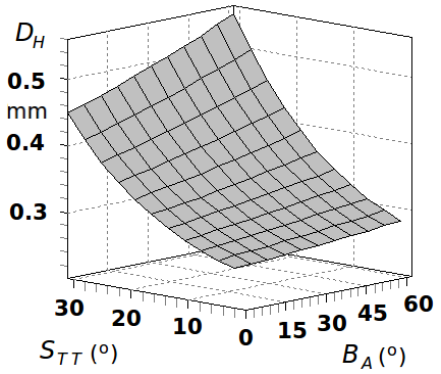

Fig. 23. The plot of relation between the dispersion D_H of hole diameter and the drill bits working part side surface tangential taper S_{TT} and the main cutting edge bevel angle in base plain B_A; centering spike maximum asymmetry angle $dB_{CS} = 11$ mm; drill bit working part side surface axial taper $S_{AT} = 5'$; axial run out of side edge $A_{RSE} = 0.19$ mm; side edge height $h_{SE} = 0.8$ mm; spindle rotational speed $n = 2880$ min^{-1}; main edge contour rake angle $G_F = 12°$; drill bit diameter $D_D = 11$ mm; height of centering spike $h_{CS} = 5.1$ mm; axial run out of main cutting edge $A_R = 0.2$ mm; radial run out of main cutting edge $R_R = 0.6$ mm; lateral stiffness of drill bits mounted in a spindle $E_L = 72$ N mm^{-1}; radial play of main cutting edge $R_P = 0.05$ mm; radial run out of centering spike $R_{RCS} = 0.55$ mm; main edge contour clearance angle $A_F = 15°$; clearance angle differences $dA_F = 2°$; rake angle differences $dG_F = 0.6°$; main cutting edge bevel angle in base plain difference $dB_A = 3°$; Brinell hardness $HB = 0.85$ MPa

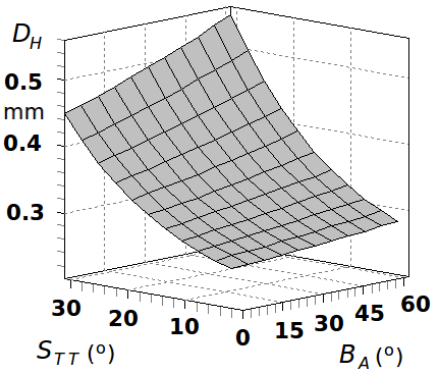

Fig. 24. The plot of relation between the dispersion of hole diameter D_H and Brinell hardness HB and the height of centering spike $h_{CS;}$ centering spike maximum asymmetry angle $dB_{CS} = 11$ mm; drill bit working part side surface axial taper $S_{AT} = 87'$; axial run out of side edge $A_{RSE} = 0$ mm; side edge height $h_{SE} = 0$ mm; spindle rotational speed $n = 2880$ min^{-1}; main edge contour rake angle $G_F = 0°$; drill bit diameter $D_D = 6$ mm; axial run out of main cutting edge $A_R = 0.2$ mm; radial run out of main cutting edge $R_R = 0.4$ mm; lateral stiffness of drill bits mounted in a spindle $E_L = 72$ N mm^{-1}; radial play of main cutting edge $R_P = 0.05$ mm; radial run out of centering spike $R_{RCS} = 0.55$ mm; main edge contour clearance angle $A_F = 43°$; clearance angle differences $dA_F = 23°$; rake angle differences $dG_F = 1.8°$; drill bits working part side surface tangential taper $S_{TT} = 0°$; main cutting edge bevel angle in base plain difference $dB_A = 12°$; main cutting edge bevel angle in base plain $B_A = 31°$

Because of interactions: $dB_{CS} \cdot E_L$, $-A_{RSE} \cdot E_L$, $R_R \cdot h_{CS}$, $R_P \cdot E_L$, $-HB \cdot h_{CS}$, $h_{CS} \cdot E_L$, $h_{CS} \cdot l_{SS}$, $h_{CS} \cdot R_P$, the dependency of the D_H upon analyzed variables may differ from those presented in Figs. from 16 to 24 for another set of independent variables.

No correlation between the D_H and following independent variables: dB_A, B_A, dl_{SS} was found.

Acceptable hole diameter dispersion D_H can be obtained by low value of: R_R, A_R and high values of A_{RSE}, h_{SE}, n, G_F. In case of high values of the HB, despite of some drill bit inaccuracies, acceptable D_H can be obtained by large values of the h_{CS}. This observation is not valid for low values of the HB (Fig. 24). It should be noted that formulas (1) and (2) are not valid for combinations of independent variables, not present in the examined incomplete experimental matrix, and, giving values ($0 > dN > 1.48$) mm and ($0.04 > D_H > 2.75$) mm.

The performed experiments show that it is possible to control, up to a certain level (standard deviation of residuals S_R), the drilling holes accuracy what condition is to identify all machining parameters.

IV. CONCLUSIONS

Experiments and analysis of the performed results allow stating that:

1. When drilling solid wood of the Scotch pine, the dependency of the shift of hole diameter dN from several machining parameters $dN = f(R_{RCS}, S_{AT}, A_{RSE}, h_{SE}$, n, $G_F, D_D, h_{CS}, A_R, R_R, E_L, R_P, A_F, dG_F, S_{TT}, HB, dB_{CS})$, can be described by formula (2), by: $S_K = 2.06$, $R = 0.89$; $R^2 = 0.80$; $S_D = 0.12$ mm.
2. The height of centering spike h_{CS}, lateral stiffness of drill bits mounted in a spindle E_L and radial run out of main cutting edge R_R, independent variables had the largest influence on the shift of hole diameter dN.
3. The largest values of the shift of hole diameter dN was observed by a minimum value of the height of centering spike h_{CS}.
4. The largest values of the shift of hole diameter dN was observed by a maximum value of the lateral stiffness of drill bits mounted in a spindle E_L and radial run out of main cutting edge R_R.
5. A decrease of the shift of hole diameter dN was observed by an increase of the: height of centering spike h_{CS}, Brinell hardness HB, drill bits working part side surface tangential taper $S_{TT}$and an decrease of the: lateral stiffness of drill bits mounted in a spindle E_L, drill bit diameter D_D, radial run out of main cutting edge R_R, as well as axial run out of main cutting edge R_R.
6. When drilling solid wood of Scotch pine, the dependency of the dispersion of hole diameter D_H from several machining parameters $D_H = f(R_{RCS}, E_L, S_{AT}, A_{RSE}, h_{SE}$, n, $G_F, D_D, h_{CS}, A_R, R_R, R_P, A_F, dA_F, dG_F, S_{TT}, B_A, HB)$, can be described by formula (2), by: $S_K = 2.06$, $R = 0.89$; $R^2 = 0.80$; $S_D = 0.12$ mm.
7. The height of centering spike h_{CS}, the lateral stiffness of drill bits mounted in a spindle E_L and the radial run out of main cutting edge R_R independent variables had the largest influence on the dispersion of hole diameter D_H.
8. The largest values of the dispersion of hole diameter D_H was observed by a minimum value of the height of centering spike h_{CS}.
9. The largest values of the dispersion of hole diameter D_H was observed by a maximum value of the lateral stiffness of drill bits mounted in a spindle E_L and the radial run out of main cutting edge R_R.
10. A decrease of the dispersion of hole diameter D_H was observed by a decrease of the following independent variables: height of centering spike h_{CS}, by $HB < 1.3$, lateral stiffness of drill bits mounted in a spindle E_L, radial run out of main cutting edge R_R, drill bit diameter D_D, drill bits working part side surface tangential taper S_{TT}, main cutting edge bevel angle in base (frontal) plain B_A, main edge contour rake angle G_F, clearance angle differences dA_F.

Acknowledgements

The author is grateful for the support of the Poznań Supercomputing and Networking Center (PCSS) calculation grant.

References

[1] K. Banshoya, Y. Kitani, *Differences in burr formation in machine through-hole boring of woo-based materials by boring tools*, Proc. of 16^{th} International Wood Machining Seminar, Matsue, Japan: 515-523, 2003.

[2] N.R. Draper, H. Smith, *Analiza regresji stosowana* (in Polish), PWN, Warszawa, 1973.

[3] W. Marzymski, *Badanie dokładności maszynowej obróbki skrawaniem drewna i wynikające przesłanki do ustalenia jednostki tolerancji*, Zeszyty Naukowe Politechniki Szczecińskiej **83** (1966).

[4] T. Ohuchi, N. Suzuki, W. Murase, *Axial deviation of hole in deep machine-boring of wood*. Proc. of 16^{th} International Wood Machining Seminar, Matsue, Japan: 524-531, 2003.

[5] B. Porankiewicz, *Problem tolerancji i pasowań dla przemysłu drzewnego* (in Polish), Rocz. AR Poznań, Prace habilitacyjne **183**, 70 (1989).

[6] TGL 24421 (1972) Masstoleranzen und Passungen für die Möbelindustrie, p. 1-35, 1972.

Appendix

Following estimators for equation (1), describing the dependence $dN = f(R_{RCS}, S_{AT}, A_{RSE}, h_{SE}, n, G_F, D_D, h_{CS}, A_R, R_R, E_L, R_P, A_F, dG_F, S_{TT}, HB, dB_{CS})$ were evaluated:

- $a_1 = -0.80121$,
- $a_2 = -0.06955$,
- $a_3 = -31.54445$,
- $a_4 = 5.04548$,
- $a_5 = 1.4082610^{-4}$,
- $a_6 = 0.02625$,
- $a_7 = 0.11193$,
- $a_8 = -1.00176$,
- $a_9 = 1.80529$,
- $a_{10} = 0.41386$,
- $a_{11} = -0.0967$,
- $a_{12} = 28.88261$,
- $a_{13} = 3.7948810^{-3}$,
- $a_{14} = -0.05196$,
- $a_{15} = 5.66612$,
- $a_{16} = -0.01345$,
- $a_{17} = 0.03073$,
- $a_{18} = -0.18505$,
- $a_{19} = -26.6443$,
- $a_{20} = -0.15406$,
- $a_{21} = 0.1583$,
- $a_{22} = -139.6572$,
- $a_{23} = 15.3268$,
- $a_{24} = -3.44529$,
- $a_{25} = 5.8214510^{-3}$,
- $a_{26} = -53.33068$,
- $a_{27} = 30.0126$,
- $a_{28} = 0.16888$,
- $a_{29} = 0.1467$.

Rounding of the values of estimators estimators for equation (2) to a number decimal digits of 5 caused acceptable deterioration of the fit less than 0.1%. Reducing number of rounding of decimal digits to 4, 3 and 2 causes unacceptable deterioration of the fit as much as: 3%, 9%, 1216% respectively.

The coefficients of relatively importance C_{RI} for estimators of equation (1) took following values:

- $C_{RI1} = 410^7$,
- $C_{RI2} = 9.710^6$,
- $C_{RI3} = 1.610^6$,
- $C_{RI4} = 98$,
- $C_{RI5} = 233$,
- $C_{RI6} = 42$,
- $C_{RI7} = 293$,
- $C_{RI8} = 2.410^6$,
- $C_{RI9} = 49$,
- $C_{RI10} = 41$,
- $C_{RI11} = 4.910^{16}$,
- $C_{RI12} = 150$,
- $C_{RI13} = 12$,
- $C_{RI14} = 3925$,
- $C_{RI15} = 68$,
- $C_{RI16} = 101$,
- $C_{RI17} = 46$,
- $C_{RI18} = 2194$,
- $C_{RI19} = 7750$,
- $C_{RI20} = 71$,
- $C_{RI21} = 385$,
- $C_{RI22} = 476$,
- $C_{RI23} = 49$,
- $C_{RI24} = 137$,
- $C_{RI25} = 15$,
- $C_{RI26} = 341$,
- $C_{RI27} = 40$,
- $C_{RI28} = 595$
- $C_{RI29} = 152$.

The following estimators for equation (2), describing the dependence $D_H = f(h_{CS}, E_L, HB, R_R, A_R, R_P, S_{AT}, S_{TT}, R_{RCS}, \mathrm{n}, h_{SE}, G_F, dG_F, A_F, dA_F, B_A, l_{SS})$ were evaluated:

- $b_1 = 4.30602$,
- $b_2 = -0.15875$,
- $b_3 = -41632.23976$,
- $b_4 = -246.62085$,
- $b_5 = -1.4886310^{-5}$,
- $b_6 = -0.05401$,
- $b_7 = 0.04447$,
- $b_8 = -8.50122$,
- $b_9 = -0.17005$,
- $b_{10} = 8.0416$,
- $b_{11} = -0.02198$,
- $b_{12} = 0.83519$,
- $b_{13} = -63.65569$,
- $b_{14} = -0.03694$,
- $b_{15} = -0.14687$,
- $b_{16} = 1.70285$,
- $b_{17} = 0.03377$,
- $b_{18} = 8.12981$,
- $b_{19} = 0.07385$,
- $b_{20} = -1.08859$,
- $b_{21} = 0.17004$,
- $b_{22} = 0.28044$,
- $b_{23} = 0.25544$,
- $b_{24} = 0.02633$,
- $b_{25} = 21.96488$,
- $b_{26} = 5.45599$,
- $b_{27} = 2.99612$,
- $b_{28} = -0.6339$,
- $b_{29} = -0.41513$,
- $b_{30} = 0.01096$,
- $b_{31} = 1.21944$,
- $b_{32} = 0.72199$,
- $b_{33} = 1.34811$,

- $b_{34} = 9.34110^{-4}$,
- $b_{35} = 0.22733$.

The number of decimal digits of 5, after rounding estimators for equation (2), causes acceptable deterioration of the fit as much as 0.4%. Reducing number of decimal digits to 4 and 3, due to rounding, causes unacceptable deterioration of the fit as much as: 22 %, 1547 % respectively.

Coefficients of relatively importance C_{RI} for estimators of equation (2) took following values:

- $C_{RI1} = 39$,
- $C_{RI2} = 5119$,
- $C_{RI3} = 7275$,
- $C_{RI4} = 0.4$,
- $C_{RI5} = 7$,
- $C_{RI6} = 679$,
- $C_{RI7} = 92$,
- $C_{RI8} = 2.0710^{16}$,
- $C_{RI9} = 2$,
- $C_{RI10} = 692$,
- $C_{RI11} = 2.0710^{16}$,
- $C_{RI12} = 317$,
- $C_{RI13} = 3.4510^{14}$,
- $C_{RI14} = 2364$,
- $C_{RI15} = 23863$,
- $C_{RI16} = 269$,
- $C_{RI17} = 119$,
- $C_{RI18} = 429$,
- $C_{RI19} = 194$,
- $C_{RI20} = 11663.8$,
- $C_{RI21} = 27$,
- $C_{RI22} = 2.110^{16}$,
- $C_{RI23} = 271$,
- $C_{RI24} = 26$,
- $C_{RI25} = 26$,
- $C_{RI26} = 26$,
- $C_{RI27} = 2.110^{16}$,
- $C_{RI28} = 2.110^{16}$,
- $C_{RI29} = 609$,
- $C_{RI30} = 702$,
- $C_{RI31} = 2.110^{16}$,
- $C_{RI32} = 1833$,
- $C_{RI33} = 310$,
- $C_{RI34} = 693$,
- $C_{RI34} = 155$.

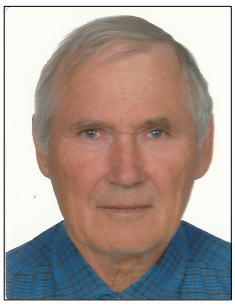

Bolesław Porankiewicz, habilitated in 2005 year at the Agricultural University of Poznań, Faculty of Wood Technology, where he also received his Doctor of Technical Science and the MSc degrees, respectively in years 1973 and 1968. In the years 2008-2011 he was employed as the contract professor at the University of Zielona Góra, Faculty of Mechanical Engineering. Since 2013 guest at Poznań University of Technology, Faculty of Machines and Transportation. Research interest: wood cutting forces, cutting accuracy, wearing of wood cutting tools, construction and exploitation of wood cutting tools and woodworking machinery.

DOI:10.12921/cmst.2015.21.01.004